REPORT DOCUMENTATION PAGE

1. REPORT DATE *(DD-MM-YYYY)*	2. REPORT TYPE	3. DATES COVERED *(From - To)*
29-09-2008	**FINAL PERFORMANCE REPORT**	Jul 2005-Sep 2008; Sep 2008

4. TITLE AND SUBTITLE
Millimeter Wave Modulators Using Quantum Dots

5a. CONTRACT NUMBER

5b. GRANT NUMBER
FA9550-05-1-0417

5c. PROGRAM ELEMENT NUMBER

6. AUTHOR(S)
Dennis W. Prather

5d. PROJECT NUMBER

5e. TASK NUMBER

5f. WORK UNIT NUMBER

7. PERFORMING ORGANIZATION NAME(S) AND ADDRESS(ES)

University of Delaware
210 Hullihen Hall
University of Delaware
Newark, DE 19716

8. PERFORMING ORGANIZATION REPORT NUMBER
ELEG332173-092908

9. SPONSORING / MONITORING AGENCY NAME(S) AND ADDRESS(ES)
Dr. Gernot Pomrenke/NE
AFOSR
875 N. Randolph St. Room 3112
Arlington, VA 22203

10. SPONSOR/MONITOR'S ACRONYM(S)

11. SPONSOR/MONITOR'S REPORT NUMBER(S)

12. DISTRIBUTION / AVAILABILITY STATEMENT
Approved for public release; distribution is unlimited.

13. SUPPLEMENTARY NOTES
None

14. ABSTRACT
In this effort electro-optic modulators for millimeter wave sensing and imaging were developed and demonstrated via design, fabrication, and experimental characterization of multi layer quantum dot structures for enhanced electro-optic interaction. Millimeter waves carry small amounts of energy inspiring us to maximize the electro-optic (EO) effect in the developed sensor material. Traditional bulk materials do not have high enough EO coefficients for this application so the goal is to custom design novel materials with optimized EO properties. InAs quantum dot samples were grown via MBE and characterized via AFM, XRD, and photoluminescence. In addition quantum dot samples were also grown in a waveguide structure, which was further incorporated in an external Mach-Zehnder Interferometer setup to characterize the electro-optic effect of the quantum dots. A reference waveguide in which bulk GaAs replaces the quantum dot materials was prepared to demonstrate the quantum dot enhancement unambiguously.

15. SUBJECT TERMS
Quantum dots, non-linear optical properties, electro-optic effect, density function theory

16. SECURITY CLASSIFICATION OF:			17. LIMITATION OF ABSTRACT	18. NUMBER OF PAGES	19a. NAME OF RESPONSIBLE PERSON
a. REPORT	b. ABSTRACT	c. THIS PAGE			Dr. Dennis W. Prather
U	U	U	UU	12	19b. TELEPHONE NUMBER *(include area code)* ***(302) 545-6611***

1 Cover Sheet

Project Title: Millimeter Wave Modulators Using Quantum Dots

Contract Number: FA9550-05-1-0417

Performing Organization

University of Delaware
Electrical and Computer Engineering Department
140 Evans Hall
Newark, DE 19716

Principal Investigator: Dr. Dennis W. Prather

Dates Covered: 1 July 2005 – 30 September 2008

2 Objectives

2.1 Develop a quantum mechanics based modeling scheme to provide physical insight regarding the enhanced non-linear optical properties in quantum dot materials.

2.2 Develop characterization techniques necessary to optimize quantum dot materials grown via MBE.

2.3 Develop a suitable device process for realizing functional millimeter wave modulators from optimized quantum dot materials.

2.4 Characterize the enhanced electro-optics properties of the synthesized materials and the devices realized using them.

3 Status of Report

We have analyzed the source of enhanced non-linear optical properties in pyramidal quantum dots from a quantum mechanical viewpoint. By applying the first principles Density Functional Theory (DFT) to model the polarization in confined systems we have identified the asymmetric effect potential introduced in pyramidal quantum dots as a source of the reported enhanced nonlinear optical effects. We have prepared a series of InAs quantum dot samples for characterization via MBE growth. Samples have been prepared for AFM, XRD and photoluminescence characterization. In addition we prepared samples with quantum dots embedded between optically confining AlGaAs layers for waveguide fabrication. The fabricated waveguides were incorporated in a modulator setup to characterize their electro-optic properties. We present the results of this characterization and compare the properties of quantum dot samples with reference bulk GaAs. We provide a discussion of the observed phenomena and methods to further enhance the non-linear optical properties in these media.

4 Accomplishments

Electro-optic based millimeter-wave detection has demonstrated sub-picowatt noise equivalent powers without cooling or low-noise amplifiers[1]. This exceptional performance enables the creation of mmW imagers without the use of expensive LNA's and can be adapted to form lensless distributed aperture imagers for high resolution. In these optical systems, the mmW signal is mapped onto an optical carrier frequency using an EO modulator. The carrier frequency is dropped using a bandpass filter and the mmW signal can be detected using a standard photodetector. These systems have already demonstrated sub-picowatt noise equivalent power. The sensitivity is limited in part by the strength of the EO material. Existing systems rely on LiNbO3 due to its large natural coefficient, ~30pm/V[2]. III-V materials, by comparison, usually offer EO coefficients of 1-2pm/V. However, it has been shown that III-V based quantum dots have the potential to significantly enhance the EO coefficient of their bulk counterparts[3,4]. III-V quantum dot materials with an enhanced EO effect could offer higher sensitivity and lower power operation while allowing monolithic integration of required detector functions.

The linear EO effect exists only in non-centrosymmetric materials due to its direct relation to the second order nonlinear optical susceptibility[2]. This susceptibility is expected to increase in pyramidal quantum dots due to the enhanced asymmetry. The density of states is increasingly limited as confinement increases toward the pinnacle of the pyramid structure. This should cause electrons in the low density of states peak to behave differently under an electric field, increasing the asymmetry inherent to a III-V crystal. We provide *ab inito* modeling results which confirm this intuition and identify a geometric region which provides optimal asymmetry. We grow InAs quantum dot samples via MBE and characterize via AFM, XRD, and photoluminescence. We also grow quantum dot samples in a waveguide structure, pattern and etch waveguides, and incorporate these waveguides in an external Mach-Zehnder Interferometer setup to characterize the electro-optic effect of the quantum dots. A reference waveguide in which bulk GaAs replaces the quantum dot materials is prepared to demonstrate the quantum dot enhancement unambiguously. Finally, a discussion is provided of the observed enhanced non-linear optical properties and limitations of the current approach.

4.1 Modeling the effect of quantum confinement on non-linear optical susceptibility

The realization of a III-V compatible material with non-linear optical susceptibility on par with or greater than leading electro-optic (EO) materials, such as $LiNbO_3$, would provide a key solution to the high speed optical modulation demands of numerous applications including mmW imaging. The strength of the second order nonlinear optical susceptibility determines a material's electro-optic coefficient, exploited in optical modulator designs for its fast response. The second order susceptibility only exists in non-centrosymmetric materials such as III-Vs. Unfortunately, the coefficient in bulk III-Vs is still an order of magnitude weaker than that in leading EO materials. Quantum dots fabricated in III-V materials (In/Al/GaAs) have demonstrated electro-optic coefficients orders of magnitude stronger than their bulk counterparts[3,4]. In this section we present *ab initio* modeling results, designed to provide physical insight regarding the enhanced non-linear properties of pyramidal quantum dots.

The nonlinear optical susceptibility of a material can be extracted by studying the dependence of polarization on electric field. We employ Density Functional Theory (DFT) to study this dependence in quantum confined systems with varying geometry. DFT solves for the ground state of a given system as a function of electron density. In this case we first solve for the ground state of a system consisting of a single electron within a two-dimensional potential well of some geometry. We then apply an external electric field and solve for the ground state in this new configuration. By monitoring the macroscopic polarization of the system under perturbations of the electric field we are able to extract a term representing the quadratic dependence. This quadratic term β, similar to $\chi^{(2)}$, acts as a metric when comparing possible enhanced EO of various geometries.

To demonstrate this approach, we consider a two-dimensional, triangular potential. The triangle shape is defined by the ratio of its height to its base. The base is set to 1nm for all geometries. A single electron is introduced within this potential.

Figure 1 shows the electron density without an electric field and with fields applied in opposite directions. The asymmetric effect of an electric field on the density is evident.

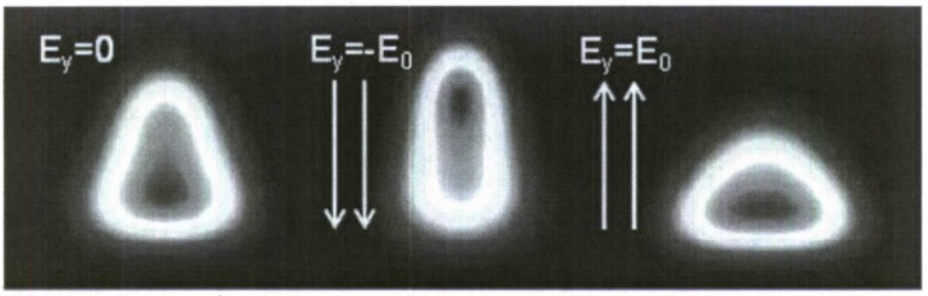

Figure 1. *Electron density in a triangular potential with and without an external electric field.*

To extract our β term, the polarization is plotted as a function of electric field. The polarization saturates for strong electric fields due to the infinite potential barrier at the boundaries of the triangle. However, in the region of small perturbations to the electric field, a quadratic dependence is observed, denoted here as β. This dependence is shown in Figure 2 (a). The β term is then extracted for triangles with aspect ratios ranging from 0.25 to 2.5, as shown in Figure 2 (b). The observed peak in the magnitude of β allows us to identify an optimal triangular geometry as having an aspect ratio between 1.5 and 1.75. A material with a triangular potential corresponding to this aspect ratio should exhibit the strongest nonlinear optical susceptibility, within the approximations of this study.

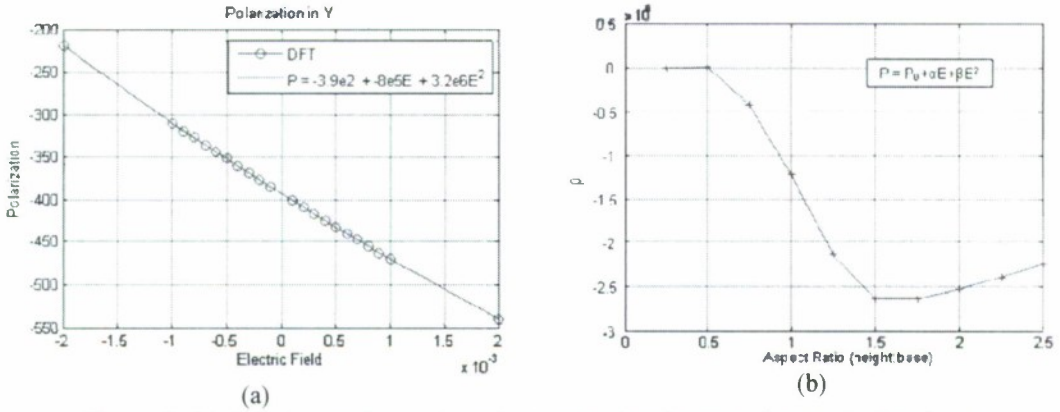

Figure 2. *(a) Polarization for a triangular potential under perturbations to the electric field, as computed by DFT, and a polynomial fit yielding a quadratic term, β. (b) β for triangles with varying aspect ratios. An optimal geometry is identified as having an aspect ratio between 1.5 and 1.75.*

In the future, a more robust study could tailor to the specific materials involved (InAs and GaAs) by incorporating their effective mass and dielectric constants. The study could also be extended to a 3D geometry in which one could study the varying effects of conical vs. pyramidal shaped potentials.

4.2 Quantum dot growth and characterization

Quantum dot samples have been grown by MBE on SVTA machine with Al, In and Ga effusion cells and As cracker. For n-type doping we used Si, for p-type doping – Be. Epi-ready GaAs:Si 2" wafers were prepared in the buffer chamber before loading on the growth manipulator. In order to remove arsenic oxide from the surface of the wafer, it was preheated on the growth stage at 630°C during 15 minutes under high As flow. The main growth process was performed at a substrate temperature of 600°C. The general InAs QD deposition involved growing 2.5 monolayer of InAs at 510°C followed by 5nm of GaAs at 410°C. The InAs deposition process was controlled by RHEED pattern conversion. Multiple layers of QDs were grown between 30 nm GaAs buffer layers.

Samples were prepared for AFM study by growing the InAs quantum dots on the surface of a GaAs substrate followed by a 2-3nm coating of GaAs, deposited to prevent surface migration of InAs. We expect that the dots embedded in a stack in the waveguide structures should be somewhat smaller in diameter and have a higher density. AFM characterization, as shown in figure 3, indicated that dots formed a lens to pyramidal shape with a base diameter of 19.9 nm and a height of 4.6. The density of quantum dots was found to be 3.5 x 10^{10} cm^{-2}.

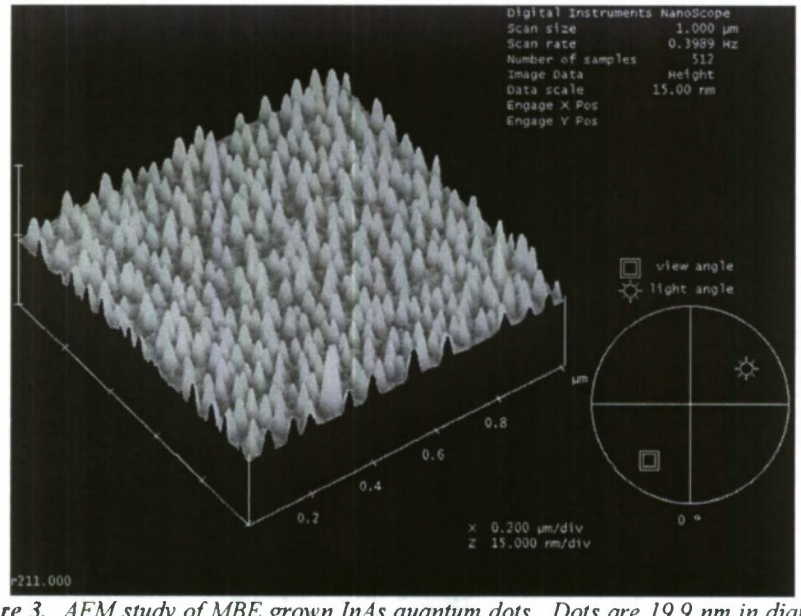

Figure 3. AFM study of MBE grown InAs quantum dots. Dots are 19.9 nm in diameter and 4.6 nm tall. The density is of dots is $3.5x10^{10}/cm^2$.

Photoluminescence studies were performed on quantum dot samples. Growth parameters such as substrate temperature and deposition time were tuned to optimize peak intensity and minimize the linewidth. The PL spectrum from an optimized quantum dot sample is shown in figure 4.

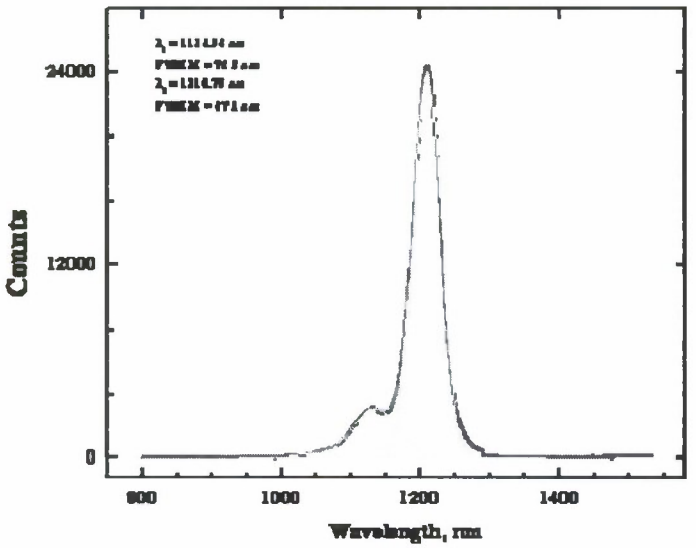

Figure 4. Photoluminescence from InAs quantum dot sample.

4.3 Quantum dot waveguides and interferometric testing

In order to measure the electro-optic coefficient for these materials we fabricated waveguides in which the optical mode is centered over the quantum dot material. The waveguide structure and associated mode profile at 1.55μm is shown in figure 5. The optical mode is largely confined to the intrinsic GaAs and QD region, between the low index AlGaAs regions. The AlGaAs consisted of 30% Al, 70% Ga resulting in an index of 3.15 compared to the bulk GaAs index of 3.3. The waveguide device included three layers of quantum dots separated by GaAs buffer layers to minimize strain. A reference sample was grown to the same specifications except that the QD layers were replaced by bulk GaAs. Low index AlGaAs regions bordering the high index GaAs and quantum dot regions provide optical confinement in the vertical direction. A 50 nm surface GaAs layer (not shown) was included to prevent oxidation of the top AlGaAs layer. The GaAs substrate is heavily n-type doped while the MBE deposited AlGaAs and GaAs regions are left undoped. Electrodes on the surface and backside of the sample allow an electric field to be applied to the intrinsic region where the optical mode is supported.

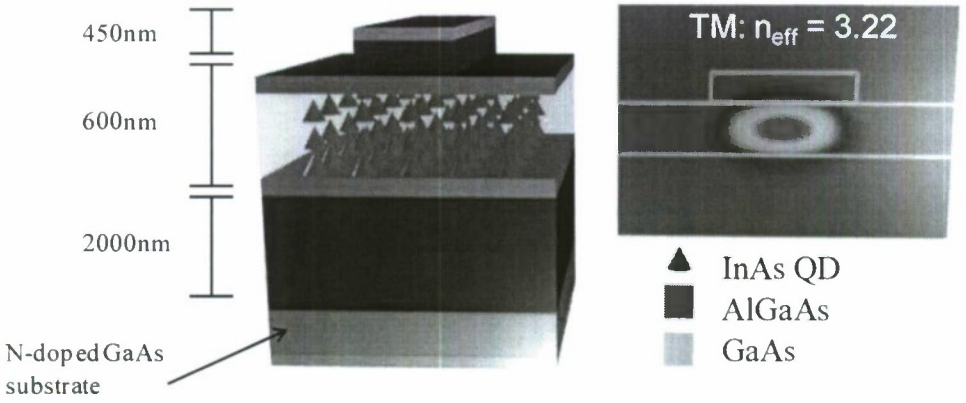

Figure 4. Schematic of MBE grown structure and waveguide structure after fabrication process. Optical confinement is achieved in the vertical direction due to the low index AlGaAs regions.

After growing the waveguide structure a chrome on glass mask was used in conjunction with a negative angle photoresist to open holes for the waveguides and electrode pad. Electrodes consisting of 5nm of Ti and 300nm of Au were deposited via E-Beam evaporation. After lift-off the Ti/Au acted as an etch mask in a Cl ICP dry etch process. Only the top 450 nm AlGaAs layer was etched, as indicated in figure 4. SEM images of the fabricated waveguides are shown in figure 5.

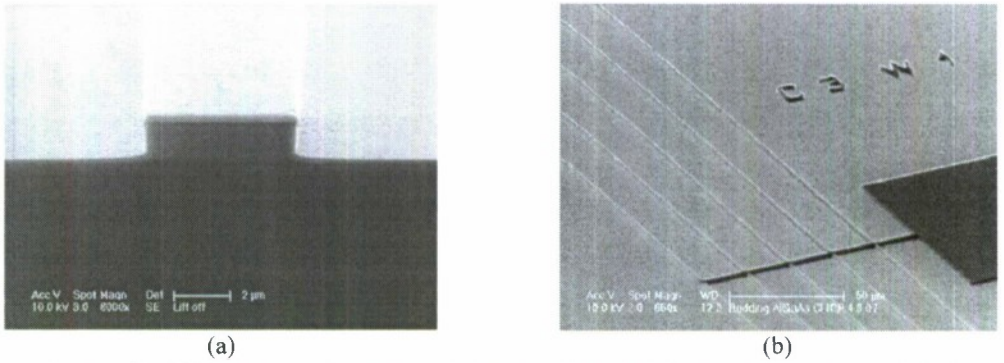

(a) (b)

Figure 5. *SEM images of quantum dot waveguides. (a) Cross section of an etched waveguide with a Ti/Au contact on its surface. (b) Image of a set of waveguides connected to an electrode pad for probing.*

The fabricated waveguide was then integrated in an external Mach-Zehnder Interferometer (MZI) setup, involving a fiber splitter and coupler, as shown in figure 6. One arm of the MZI includes the quantum dot waveguide which is coupled in and out of using tapered polarization maintaining fibers; the other arm is all fiber and connects directly from the splitter to the coupler. A 1.55 μm laser source is used and the output of the fiber coupler is measured using an InGaAs detector. The sample is mounted on a metal stage which is grounded. The top electrode pad is contacted using a 1 μm diameter tungsten probe tip. The InGaAs detected optical signal is studied by oscilloscope in conjunction with the applied AC signal to analyze the modulator efficiency and extract an electro-optic coefficient.

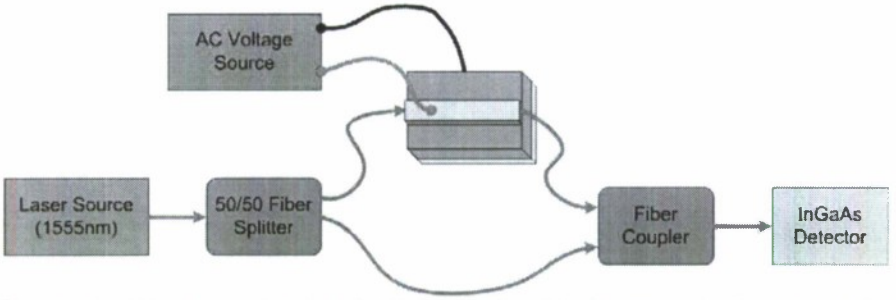

Figure 6. *Schematic of external Mach-Zehnder Interferometer test setup used to measure electro-optic coefficients. All fibers are polarization maintaining.*

To ensure that we are measuring an effect due to an applied electric field, rather than carriers passing through the waveguide, we report a typical IV curve in figure 7. IV curves were taken for each sample to identify a voltage range such that the current remained less than $1 mA/cm^2$. Subsequent testing was confined to this region.

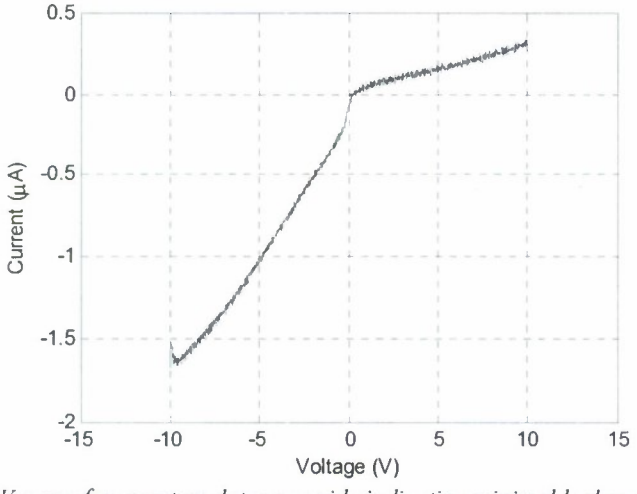

Figure 7: *IV curve for quantum dot waveguide indicating minimal leakage current within the range of +10 to -10V.*

4.4 Results and Analysis

The EO coefficient determines the amount of change in refractive index under an applied electric field as,

$$n = n_0 + \tfrac{1}{2} n_0^3 r_{41} E \qquad (1)$$

where E is the electric field, n_0 is the original refractive index, and r_{41} is the non-zero EO coefficient for cubic $\bar{4}3m$ crystals (which includes GaAs and InAs). In the external MZI setup, the effect of this is to introduce a voltage dependent phase change in the quantum dot waveguide arm. This phase difference relative to the external fiber arm will modulate the intensity when the arms are recombined in the fiber coupler. This modulated intensity is overlaid on an oscilloscope with the voltage signal. Unfortunately, since we

do not know the initial phase difference at 0V applied, and since this phase difference is likely to change over time due to uncertainty in the fiber coupling, we rely on driving the waveguide through a π phase shift within a single voltage sweep. This π phase shift manifests itself as the optical signal changing direction twice within a single voltage sweep. The voltage corresponding to the distance between the two inflection points is defined as $V\pi$ and can be related to the electro-optic coefficient as[5]

$$V_\pi = \frac{\lambda d}{l n_0^3 r_{41}}, \tag{2}$$

where λ is the wavelength, d is the distance across which the voltage is applied and l is the length of modulation. To measure $V\pi$ we take capture an oscilloscope reading and average the $V\pi$ for each voltage sweep, as shown in figure 8.

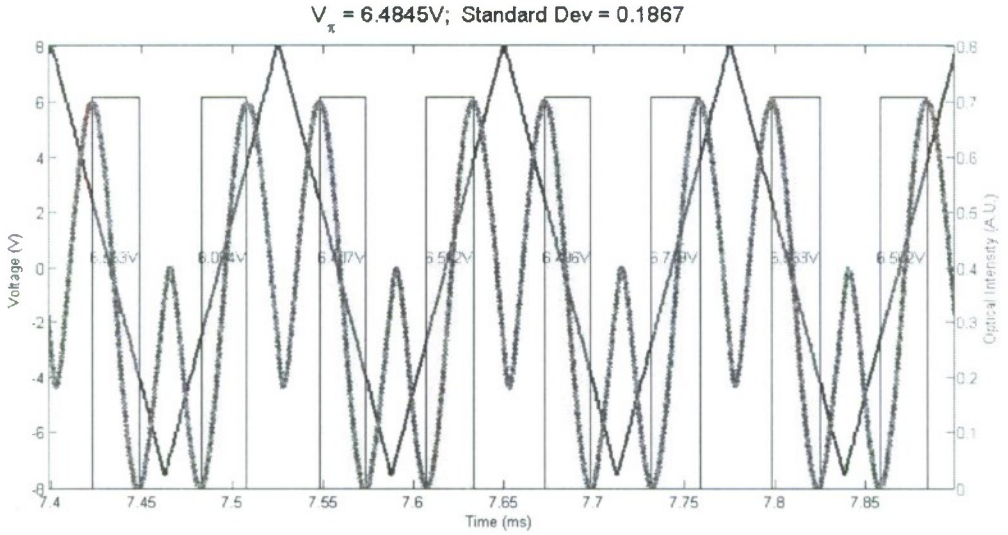

Figure 8: *Oscilloscope reading of $V\pi$ modulation for a typical quantum dot waveguide. The triangle signal in blue is the AC voltage signal, ranging from -8V to +8V. The optical signal is overlaid in red. $V\pi$ measurements correspond to the voltage change between two inflection points in the optical signal within a single voltage sweep, as highlighted in green.*

We take three of these measurements at frequencies of 1, 2, 4 and 8kHz. The $V\pi$ we use to extract an EO coefficient is the average of these twelve oscilloscope capture. The modulation is not expected to change within this frequency range, and indeed the measurements for the quantum dot and reference bulk sample exhibit a standard deviation of 3.4% and 2% respectively. We normalize the measured values to the device length d equal to 1cm, yielding $V\pi$/cm for the quantum dot sample of 7.51 and for the bulk GaAs sample of 8.21. In figure 9 we present the measured phase change as a function of voltage for the twelve quantum dot and reference GaAs measurements. The enhanced modulation effect is evident.

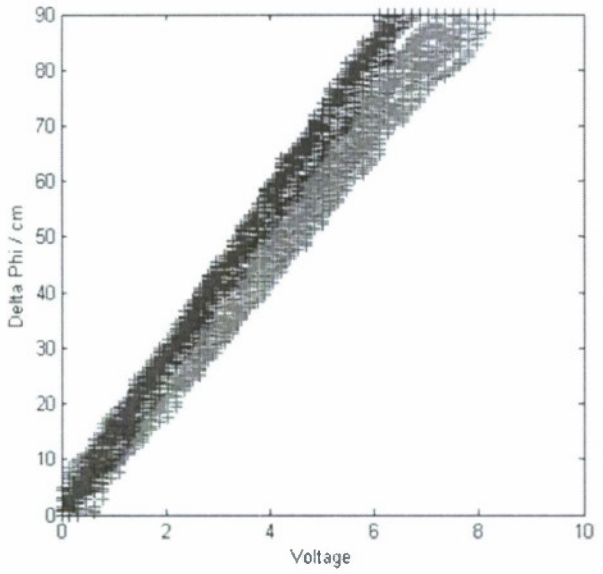

Figure 9: *The phase change as a function of voltage for a quantum dot and reference GaAs sample are compared. The blue data points indicate the quantum dot sample while the red data points indicate the reference GaAs sample.*

To extract the EO coefficient for the individual quantum dot layers we first generalize our expression for Vπ as

$$V_\pi = \frac{\lambda d}{l}\left(\sum_i \Gamma_i n_i^3 r_i\right)^{-1}. \tag{3}$$

In this expression we account for each electro-optic material separately by associating with it an optical mode overlap factor Γ_i. These overlap factors are calculated using a two-dimensional mode solver. The EO coefficients for the GaAs and AlGaAs layer are fit for the reference sample first. It is found that these coefficients are in good agreement with those reported in the literature[2]. The quantum dot EO coefficient is then the only remaining variable when fitting the corresponding Vπ measurement. The confinement factors and EO coefficients are reported in table I.

Table I

Material	n_0	Γ	r_{41}
$Al_{0.3}Ga_{0.7}As$	3.15	0.12	1.41pm/V
GaAs	3.3	0.87	1.64pm/V
InAs QD	3.3	0.013	13.5pm/V

We find that the EO coefficient for the quantum dot material is 13.5pm/V, an order of magnitude stronger than the EO coefficient in the bulk III-V materials. We attribute this enhancement to the asymmetric potential as discussed above in section 4.1. While we are encouraged by the enhanced performance of the quantum dot material, we note that due to the small overlap of the optical mode with the QDs, the overall modulator efficiency experiences only a moderate improvement. Indeed, if we use an effective index of 3.22

in equation 2, we can extract an effective EO coefficient for the reference and quantum dot samples of 1.7pm/V and 1.85pm/V. To improve the modal overlap with the quantum dot material, we grew and fabricated devices with as many as 20 layers of quantum dots embedded in the GaAs region. Unfortunately, the additional layers did not significantly affect the overall modal performance of the modulator. We suspect that this may be due to strain in the additional layers. Furthermore, referring back to our modeling of a pyramidal potential in section 4.1, we found that an optimal geometry in two-dimensions should have an aspect ratio of ~1.5:1. Based on our AFM measurements, the devices we have fabricated consist of quantum dots with an aspect ratio of ~0.25:1. The model predicts very minimal enhanced EO properties for such a low aspect ratio. In the future, realization of III-V based modulators seeking an enhanced modal EO coefficient might focus on increasing the aspect ratio of the quantum dots and the overlap with the optical mode.

5 Personnel Supported

Faculty : Prof. Dennis Prather
Post Doctorate:
Graduate students: Brandon Redding

6 Publications

Proceedings SPIE: Optics & Photonics "Design, fabrication, and testing of enhanced EO materials for mmW modulators," B. Redding, N. Faleev, X. Long, T. Creazzo, S. Shi, D. Prather, August, 2007.

CLEO/QELS "Enhanced Electro-optic effect in InAs/GaAs Quantum Dots," B. Redding, X. Long, N. Faleev, S. Shi, D. Prather, May, 2008.

7 Interactions/Transitions

None

8 New Discoveries

None

9 Honors/Awards

None

10 References

1. C. Schuetz, J. Murakowski, G. Schneider, and D. Prather, "Radiometric millimeter-wave detection via optical upconversion and carrier suppression," IEEE Trans. Mircowave Theory Tech. **53**, 1732, 2005.
2. M. Veithen, X. Gonze, and Ph. Ghosez, "Nonlinear optical susceptibilities, Raman efficiencies, and electro-optic tensors from first-principles density functional perturbation theory," Phys. Rev. B **71**, 125107, 2005.
3. S. Ghosh, A. Lenihan, M. Dutt, O. Qasaimeh, D. Steel, P. Bhattacharya, "Nonlinear optical and electro-optic properties of InAs/GaAs self-organized quantum dots," J. Vac. Sci. Tech. B **19**, 1455, 2001.
4. J. Tatebayashi, R. Laghumavarapu, N. Nuntawong, and D. Huffaker, "Measurement of electro-optic coefficients of 1.3um self-assembled InAs/GaAs quantum dots," Electron. Lett. **43**, 410, 2007.
5. A. Yariv, *Optical Electronics in Modern Communications*, Oxford University Press, New York, 2001.
6. M. Koshiba, Y. Tsuji, and M. Nishio, "Finite-element modeling of broad-band traveling-wave optical modulators," IEEE Trans. Microwave Theory Tech. **47**, 1627, 1999.